INSTITUTE OF PHYSICS PUBLISHING JOURNAL OF PHYSICS B: ATOMIC, MOLECULAR AND OPTICAL PHYSICS

J. Phys. B: At. Mol. Opt. Phys. **34** (2001) 639–645 www.iop.org/Journals/jb PII: S0953-4075(01)18389-6

A comparison of theoretical line intensity ratios for Ni XII with extreme ultraviolet observations from the JET tokamak

F P Keenan[1], G J J Botha[1], A Matthews[1], K D Lawson[2], K L Bell[3], C A Ramsbottom[3], I H Coffey[2] and M O'Mullane[2]

[1] Department of Pure and Applied Physics, The Queen's University of Belfast, Belfast BT7 1NN, UK
[2] Culham Science Centre, Abingdon, Oxfordshire OX14 3DB, UK
[3] Department of Applied Mathematics and Theoretical Physics, The Queen's University of Belfast, Belfast BT7 1NN, UK

Received 28 October 2000, in final form 27 November 2000

Abstract

Recent R-matrix calculations of electron impact excitation rates in Ni XII are used to derive the emission line ratios $R_1 = I(154.17\ \text{Å})/I(152.15\ \text{Å})$, $R_2 = I(152.95\ \text{Å})/I(152.15\ \text{Å})$ and $R_3 = I(160.55\ \text{Å})/I(152.15\ \text{Å})$. This is the first time (to our knowledge) that theoretical emission line ratios have been calculated for this ion. The ratios are found to be insensitive to changes in the adopted electron density (N_e) when $N_e \geqslant 5 \times 10^{11}$ cm^{-3}, typical of laboratory plasmas. However, they do vary with electron temperature (T_e), with for example R_1 and R_3 changing by factors of 1.3 and 1.8, respectively, between $T_e = 10^5$ and 10^6 K. A comparison of the theoretical line ratios with measurements from the *Joint European Torus* (JET) tokamak reveals very good agreement between theory and observation for R_1, with an average discrepancy of only 7%. Agreement between the calculated and experimental ratios for R_2 and R_3 is less satisfactory, with average differences of 30 and 33%, respectively. These probably arise from errors in the JET instrument calibration curve. However, the discrepancies are smaller than the uncertainties in the R_2 and R_3 measurements. Our results, in particular for R_1, provide experimental support for the accuracy of the Ni XII line ratio calculations, and hence for the atomic data adopted in their derivation.

1. Introduction

Emission lines due to transitions in ions of the chlorine isoelectronic sequence have been detected from a wide variety of astronomical sources, as well as in laboratory plasmas (Keenan 1996). These transitions may be used to determine the electron temperature and/or density of the emitting region via diagnostic line ratios, although to calculate these reliably, accurate atomic data must be employed, especially for electron impact excitation rates (Mason and

0953-4075/01/040639+07$30.00

Monsignori-Fossi 1994). To date, most observational and theoretical effort on Cl-like ions has been devoted to Fe x, for which several calculations of electron impact excitation rates have been undertaken (see, e.g., Mason 1994, Mohan *et al* 1994, Bhatia and Doschek 1995).

Until recently, there were no excitation rate calculations available for Cl-like Ni xii, apart from that of Pelan and Berrington (1995) for the $3s^2 3p^5\ ^2P_{1/2} - 3s^2 3p^5\ ^2P_{3/2}$ ground state fine-structure transition. However, Matthews *et al* (1998) have calculated highly accurate electron excitation rates for a large number of transitions in Ni xii using the *R*-matrix code (Berrington *et al* 1987). In this paper we present for the first time (to our knowledge) theoretical emission line ratios for Ni xii, determined using the Matthews *et al* (1998) atomic data. These are compared with extreme ultraviolet observations from the *Joint European Torus* (JET) tokamak, to investigate their usefulness as diagnostics for laboratory plasmas.

2. Atomic data and theoretical line ratios

The model ion adopted for Ni xii consisted of the 14 energetically lowest *LS* states, namely $3s^2 3p^5\ ^2P$, $3s 3p^6\ ^2S$, $3s^2 3p^4\ (^3P)\ 3d\ ^4D$, $3s^2 3p^4\ (^1D)\ 3d\ ^2P$, $3s^2 3p^4\ (^3P)\ 3d\ ^4F$, $3s^2 3p^4\ (^3P)\ 3d\ ^4P$, $3s^2 3p^4\ (^1D)\ 3d\ ^2D$, $3s^2 3p^4\ (^3P)\ 3d\ ^2F$, $3s^2 3p^4\ (^1D)\ 3d\ ^2G$, $3s^2 3p^4\ (^1D)\ 3d\ ^2F$, $3s^2 3p^4\ (^1S)\ 3d\ ^2D$, $3s^2 3p^4\ (^1D)\ 3d\ ^2S$, $3s^2 3p^4\ (^3P)\ 3d\ ^2P$ and $3s^2 3p^4\ (^3P)\ 3d\ ^2D$. This gives a total of 31 levels when the fine-structure splitting is included. Energies of all these levels were taken from Fawcett (1987).

Electron impact excitation rates for transitions in Ni xii were taken from Matthews *et al* (1998), while for Einstein *A* coefficients the calculations of Fawcett (1987) and Nussbaumer (1976) were adopted. As has been discussed by, for example, Seaton (1964), proton excitation may be important for transitions with small excitation energies, i.e. fine-structure transitions such as those within the $2s^2 2p\ ^2P$ and $2s 2p^2\ ^4P$ terms of boron-like ions (Foster *et al* 1997). However, test calculations for Ni xii setting the proton excitation rates for fine-structure transitions equal to the corresponding electron rates, or ten times these values, had a negligible effect on the level populations, showing this atomic process to be unimportant for this ion, at least at the electron temperatures and densities under consideration.

Using the atomic data discussed above in conjunction with the *atomic data and analysis structure* (ADAS) code (Summers 1994), relative Ni xii level populations and hence emission line strengths were calculated for a range of electron temperatures (T_e) and densities (N_e). The following assumptions were made in the calculations: (i) that ionization to and recombination from other ionic levels is slow compared with bound–bound rates, (ii) that photoexcitation and induced de-excitation rates are negligible in comparison with the corresponding collision rates, and (iii) that all transitions are optically thin. Further details of the procedures involved may be found in Summers (1994).

3. Experimental line ratios

The intensities of Ni xii lines were measured from spectra of the JET tokamak. JET is currently the largest tokamak experiment in the world. The project was designed with the objectives of obtaining and studying plasmas in conditions and dimensions approaching those needed in a fusion reactor (Rebut *et al* 1987). JET has overall dimensions of about 15 m in diameter and 12 m in height, and the *D*-shaped vacuum vessel is of major radius $R_0 = 2.96$ m, with minor radii of $a = 1.25$ m (horizontal) and $b = 2.10$ m (vertical). The toroidal component of the magnetic field is generated by 32 *D*-shaped coils equally spaced around the torus and enclosing the vacuum vessel, and at the plasma centre the maximum field strength is 3.45 T. A

Table 1. Characteristics of the JET pulses studied.

JET pulse	Time (s)	Regime	Additional heating	log T_e	N_e (10^{13} cm^{-3})
31 275	58.27	Ohmic	—	5.2	13.0
30 780	41.58	L-mode	LHCD	5.4	3.0
31 273	61.08	L-mode	NBI	5.4	9.0
31 327	52.20	L-mode	NBI	5.4	5.0
31 272	59.50	H-mode	NBI	6.1	10.0
31 275	57.70	H-mode	NBI	6.1	14.0
31 798	49.06	H-mode	LHCD/NBI/ICR	6.1	7.0
31 798	49.59	H-mode	LHCD/NBI/ICR	6.1	7.2
31 798	49.81	H-mode	LHCD/NBI/ICR	6.1	7.4

plasma current of up to 7 MA is produced by transformer action using an 8-limbed magnetic circuit. Around the centre limb of the magnetic circuit is a set of coils, which acts as the primary winding, the plasma itself acting as the secondary. Poloidal coils situated around the outside of the vacuum vessel are used to shape and position the plasma.

In table 1 we list the characteristics of the JET pulses studied in this paper. These include the time into the pulse a spectrum was taken, and the regime under which the plasma was operating at that time, namely: ohmic—no additional heating (steady-state plasma); L-mode—a low confinement mode with additional heating; H-mode—a high confinement mode with additional heating and steep edge gradients. The sources of additional heating are summarized in table 1, and include lower hybrid current drive (LHCD), neutral beam injection (NBI) and ion cyclotron resonance (ICR) heating. Also listed in table 1 are the logarithmic electron temperature and line-of-sight electron density in each pulse, measured from probes within the plasma. These temperature and density estimates should be accurate to ± 0.2 dex and $\pm 10\%$, respectively.

Spectra of the JET pulses listed in table 1 were recorded using a 2 m extreme grazing-incidence (Schwob–Fraenkel) spectrometer (Schwob *et al* 1987), equipped with a 600 grooves mm^{-1} grating and two microchannel-plate image intensifier–convertor detector systems, fibre-optically coupled to 1024-element photodiode arrays. These detectors are moveable along the Rowland circle, and cover 20–60 Å sections of spectra, depending on the wavelength. We observed the 148–164 Å wavelength region at a spectral resolution of 0.2 Å (FWHM). These spectra were wavelength calibrated using, as standards, the emission lines of species which are intrinsic to the plasma, including C V 148.50 Å and Ni XXVI 157.50 Å (see Denne *et al* (1989) for more details). The following Ni XII emission lines were identified and measured:

- the $3s^2 3p^5\ ^2P_{3/2} - 3s^2 3p^4\ (^3P)\ 3d\ ^2P_{1/2} + 3s^2 3p^5\ ^2P_{3/2} - 3s^2 3p^4\ (^3P)\ 3d\ ^2D_{5/2}$ line blend at 152.15 Å;
- the $3s^2 3p^5\ ^2P_{1/2} - 3s^2 3p^4\ (^3P)\ 3d\ ^2D_{3/2}$ transition at 152.95 Å;
- the $3s^2 3p^5\ ^2P_{3/2} - 3s^2 3p^4\ (^3P)\ 3d\ ^2P_{3/2}$ transition at 154.17 Å;
- the $3s^2 3p^5\ ^2P_{3/2} - 3s^2 3p^4\ (^1D)\ 3d\ ^2S_{1/2}$ transition at 160.55 Å;

where the line identifications are from Goldsmith and Fraenkel (1970) and Gabriel *et al* (1966). In figure 1 we show the spectrum of a pulse, to illustrate the quality of the observational data.

4. Results and discussion

In figures 2–4 we plot the theoretical Ni XII emission line ratios:

- $R_1 = I(154.17\ \text{Å})/I(152.15\ \text{Å})$

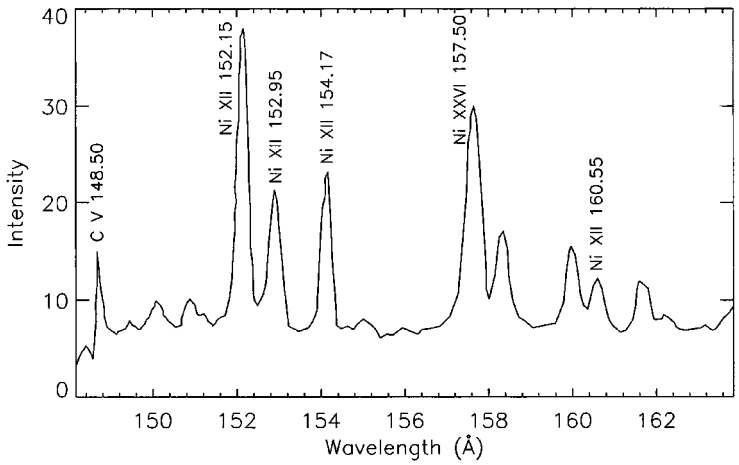

Figure 1. Spectrum of JET pulse 31 798, taken 49.06 s into the pulse, in the wavelength range 148–164 Å. Several Ni XII lines are identified in the spectrum, as well as transitions of C V and Ni XXVI.

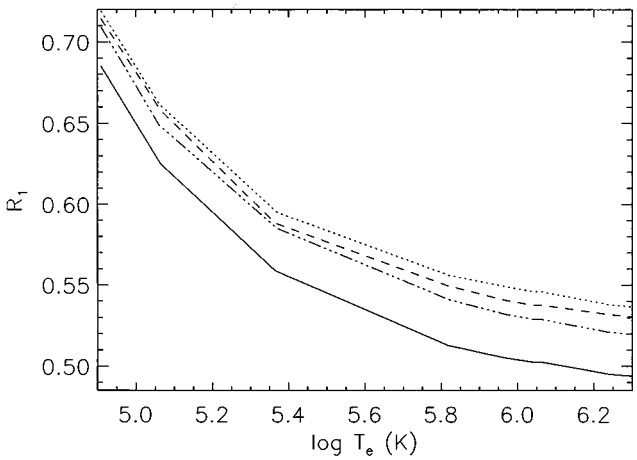

Figure 2. The theoretical Ni XII emission line ratio $R_1 = I(3s^23p^5\ ^2P_{3/2} - 3s^23p^4\ (^3P)\ 3d\ ^2P_{3/2})/I(3s^23p^5\ ^2P_{3/2} - 3s^23p^4\ (^3P)\ 3d\ ^2P_{1/2} + 3s^23p^5\ ^2P_{3/2} - 3s^23p^4\ (^3P)\ 3d\ ^2D_{5/2}) = I(154.17\,\text{Å})/I(152.15\,\text{Å})$, where I is in photon units, plotted as a function of electron temperature at electron densities of $N_e = 10^{10}$ cm^{-3} (full curve), $N_e = 5 \times 10^{10}$ cm^{-3} (chain curve), $N_e = 10^{11}$ cm^{-3} (broken curve), and $N_e = 5 \times 10^{11}$ cm^{-3} (dotted curve). We note that the theoretical ratios for $N_e > 5 \times 10^{11}$ cm^{-3} are coincident with those for $N_e = 5 \times 10^{11}$ cm^{-3}.

- $R_2 = I(152.95\ \text{Å})/I(152.15\ \text{Å})$
- $R_3 = I(160.55\ \text{Å})/I(152.15\ \text{Å})$

as a function of electron temperature for a range of electron densities between $N_e = 10^{10}$ and 5×10^{11} cm^{-3}, noting that the results are insensitive to variations in the density for $N_e \geqslant 5 \times 10^{11}$ cm^{-3}. Given errors in the adopted atomic data of typically $\pm 10\%$ (see references in section 2), we would expect the theoretical ratios to be accurate to better than 20%.

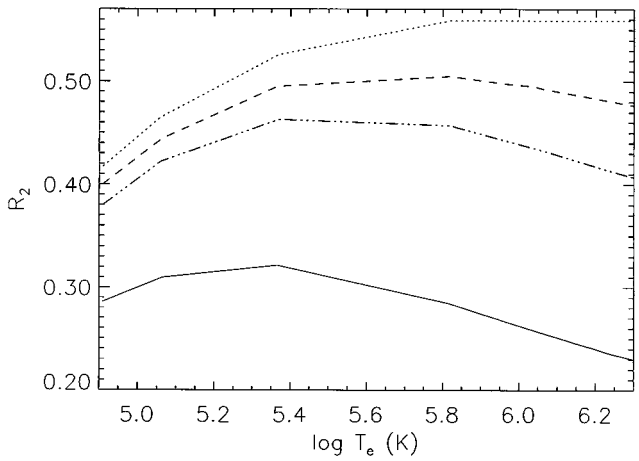

Figure 3. Same as figure 2 but for $R_2 = I(3s^2 3p^5\ ^2P_{1/2} - 3s^2 3p^4\ (^3P)\ 3d\ ^2D_{3/2})/I(3s^2 3p^5\ ^2P_{3/2} - 3s^2 3p^4\ (^3P)\ 3d\ ^2P_{1/2} + 3s^2 3p^5\ ^2P_{3/2} - 3s^2 3p^4\ (^3P)\ 3d\ ^2D_{5/2}) = I(152.95\ \text{Å})/I(152.15\ \text{Å})$.

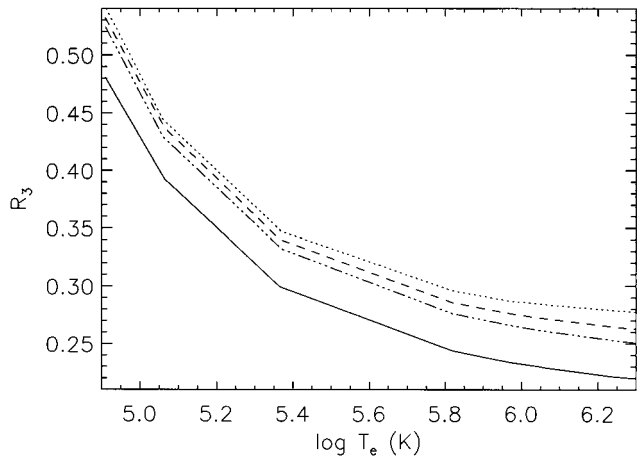

Figure 4. Same as figure 2 but for $R_3 = I(3s^2 3p^5\ ^2P_{3/2} - 3s^2 3p^4\ (^1D)\ 3d\ ^2S_{1/2})/I(3s^2 3p^5\ ^2P_{3/2} - 3s^2 3p^4\ (^3P)\ 3d\ ^2P_{1/2} + 3s^2 3p^5\ ^2P_{3/2} - 3s^2 3p^4\ (^3P)\ 3d\ ^2D_{5/2}) = I(160.55\ \text{Å})/I(152.15\ \text{Å})$.

An inspection of figures 2–4 reveals that R_1 and R_3 are sensitive to variations in the adopted electron temperature, with for example at $N_e = 10^{11}$ cm^{-3} the former varying by 30% between $T_e = 10^5$ and 10^6 K, while the latter changes by a factor of 1.8 over the same temperature interval. Hence in principle the ratios should be useful T_e diagnostics, provided that $N_e \geqslant 5 \times 10^{11}$ cm^{-3} (as is the case with the current JET observations; see section 3 and table 1), so that the density sensitivity is removed. However, R_2 does not vary monotonically with T_e, but rather reaches a maximum at $\log T_e \simeq 5.8$, and only provides a useful diagnostic at low values of T_e.

In table 2 we summarize the experimental values of R_1, R_2 and R_3 for the JET pulses listed in table 1. The R_1 measurements should be reliable to 10%, as the 152.15 and 154.17 Å lines are close together (reducing uncertainties associated with instrument calibration), and are both strong. However, the experimental R_2 and R_3 ratios are only accurate to 25 and 50%,

Table 2. Observed and theoretical Ni XII emission line ratios.

		R_1		R_2		R_3	
JET pulse	Time (s)	Observed	Theory[a]	Observed	Theory[a]	Observed	Theory[a]
31 275	57.70	0.55	0.54	0.36	0.56	0.23	0.28
30 780	41.58	0.49	0.59	0.37	0.53	—	0.34
31 273	61.08	0.59	0.59	0.38	0.53	0.23	0.34
31 327	52.20	0.69	0.59	0.44	0.53	0.22	0.34
31 272	59.50	0.59	0.54	0.34	0.56	0.16	0.28
31 275	58.27	0.60	0.63	0.39	0.49	0.19	0.40
31 798	49.06	0.53	0.54	0.41	0.56	0.18	0.28
31 798	49.59	0.61	0.54	0.39	0.56	0.23	0.28
31 798	49.81	0.57	0.54	0.30	0.56	0.19	0.28

[a] Theoretical ratios derived from figures 2–4 using the JET pulse plasma parameters in table 1.

respectively. The large uncertainty for R_3 is due in part to the weakness of the 160.55 Å line (see figure 1), but the main source of error for this ratio (and also for R_2) is the reliability of the instrument calibration, which is a strong function of wavelength separation.

Unfortunately, the errors in the observed R_1, R_2 and R_3 ratios are such that they cannot be used to estimate reliable values of T_e from the diagnostic calculations in figures 2–4. Instead, we compare the measured ratios with theoretical values, which have been calculated for the JET pulse plasma parameters summarized in table 1. These theoretical ratios are listed in table 2.

An inspection of table 2 reveals that agreement between observation and theory for R_1 is excellent, with a typical discrepancy of only 7%. In addition, we note that the average observed value of R_1 is 0.58 ± 0.05, compared to the mean theoretical ratio of 0.57.

For R_2 and R_3, the agreement between theory and experiment is less satisfactory, with average discrepancies of 30 and 33%, respectively. The mean observed ratios are $R_2 = 0.38 \pm 0.04$ and $R_3 = 0.20 \pm 0.03$, compared with theoretical estimates of 0.54 (R_2) and 0.31 (R_3). However, we note that these discrepancies are systematic, not random, as would be expected if the differences were simply due to errors arising from, for example, low counts in the emission lines. An inspection of table 2 reveals that all of the observed R_2 and R_3 ratios are smaller than the theoretical results. In contrast, for R_1 there are five observations larger than theory, and three smaller.

Systematic errors between the measured and calculated R_2 and R_3 ratios could be due to either (a) errors in the adopted atomic data, or (b) systematic errors in the measurements, most likely arising from uncertainties in the instrument calibration. However, it is highly unlikely that there would be errors in the atomic data for the transitions in the R_2 and R_3 ratios, and not in R_1 (for which agreement between theory and observation is excellent), especially as all of the emission lines considered are within the same configuration. In addition, an inspection of tables 1 and 2 reveals that there is no trend of increasing discrepancy between theory and observation with increasing temperature. This might be expected if there were systematic errors in the atomic data, as for example the reliability of electron impact excitation rates generally decreases with increasing T_e (Matthews *et al* 1998).

It therefore appears very likely that the discrepancies for R_2 and R_3 arise from systematic errors in the line ratio measurements, due to uncertainties in the instrument calibration. However, we note that these discrepancies are still smaller than the uncertainties in the R_2 and R_3 measurements (see above).

The good agreement found between the observed Ni XII R_1 line ratios and the calculated values, and the satisfactory agreement for R_2 and R_3, provides experimental support for the accuracy of the theoretical results, and hence for the atomic data adopted in their derivation. This indicates that the Ni XII line ratio diagnostics may be applied with confidence to the analysis of remote plasma sources for which no independent estimates of temperature or density are available. In particular, we note that, although the R_1, R_2 and R_3 ratios are density insensitive for $N_e \geqslant 5 \times 10^{11}$ cm^{-3}, typical of laboratory plasmas, they do vary with N_e at lower densities. The solar transition region has $N_e \simeq 10^9$–10^{11} cm^{-3} at temperatures where Ni XII should be formed in ionization equilibrium (Keenan *et al* 1991). Hence the Ni XII line ratios may provide useful N_e diagnostics for the Sun, using for example high quality spectra from the *solar and heliospheric observatory* (SOHO) mission (Harrison *et al* 1997). There is also the possibility of detecting Ni XII features in stellar observations, from for example the *Chandra* and *Extreme Ultraviolet Explorer* (EUVE) satellites (Jordan 1996). We hope to undertake such a search in the future.

Acknowledgments

GJJB, AM and CAR are grateful to PPARC for financial support. This paper was also supported by the Royal Society and the Leverhulme Trust.

References

Berrington K A, Burke P G, Butler K, Seaton M J, Storey P J, Taylor K T and Yan Yu 1987 *J. Phys. B: At. Mol. Phys.* **20** 6379
Bhatia A K and Doschek G A 1995 *At. Data Nucl. Data Tables* **60** 97
Denne B, Hinnov E, Ramette J and Saoutic B 1989 *Phys. Rev.* A **40** 1488
Fawcett B C 1987 *At. Data Nucl. Data Tables* **36** 151
Foster V J, Keenan F P and Reid R H G 1997 *At. Data Nucl. Data Tables* **67** 99
Gabriel A H, Fawcett B C and Jordan C 1966 *Proc. Phys. Soc.* **87** 825
Goldsmith S and Fraenkel B S 1970 *Astrophys. J.* **161** 317
Harrison R A *et al* 1997 *Solar Phys.* **170** 123
Jordan C 1996 *IAU Colloquium* **152** 81
Keenan F P 1996 *Space Sci. Rev.* **75** 537
Keenan F P, Dufton P L, Boylan M B, Kingston A E and Widing K G 1991 *Astrophys. J.* **373** 695
Mason H E 1994 *At. Data Nucl. Data Tables* **57** 305
Mason H E and Monsignori-Fossi B C 1994 *Astron. Astrophys. Rev.* **6** 123
Matthews A, Ramsbottom C A, Bell K L and Keenan F P 1998 *At. Data Nucl. Data Tables* **70** 41
Mohan M, Hibbert A and Kingston A E 1994 *Astrophys. J.* **434** 389
Nussbaumer H 1976 *Astron. Astrophys.* **48** 93
Pelan J and Berrington K A 1995 *Astron. Astrophys. Suppl.* **110** 209
Rebut P H *et al* 1987 *Fusion Technol.* **11** 11
Schwob J L, Wouters A W, Suckewer S and Finkenthal M 1987 *Rev. Sci. Instrum.* **58** 1601
Seaton M J 1964 *Mon. Not. R. Astron. Soc.* **127** 191
Summers H P 1994 *Atomic Data and Analysis Structure User Manual* JET–IR(94)06